AGU ADVANCING EARTH AND SPACE SCIENCES

Space Weather

RESEARCH ARTICLE
10.1029/2024SW004216

Enhanced Spacecraft Charging Risks by Interplanetary Alfvén Waves During Geomagnetic Storms

Hui Li[1,2,3], **Xiaodong Liu**[1,2,3], **and Chi Wang**[1,2,3]

[1]State Key Laboratory of Space Weather, National Space Science Center, CAS, Beijing, China, [2]Key Laboratory of Solar Activity and Space Weather, National Space Science Center, CAS, Beijing, China, [3]University of Chinese Academy of Sciences, Beijing, China

Key Points:

- During geomagnetic storm recovery, geosynchronous satellites face higher surface charging risks below −4,000 V than during the main phase
- Interplanetary Alfvén waves and their amplitudes significantly increase spacecraft surface charging
- Increased electron temperatures during Alfvén waves correlate with enhanced spacecraft charging risk

Correspondence to:
H. Li,
hli@nssc.ac.cn

Citation:
Li, H., Liu, X., & Wang, C. (2025). Enhanced spacecraft charging risks by interplanetary Alfvén waves during geomagnetic storms. *Space Weather*, *23*, e2024SW004216. https://doi.org/10.1029/2024SW004216

Received 13 OCT 2024
Accepted 27 AUG 2025

Author Contributions:
Conceptualization: Hui Li
Data curation: Xiaodong Liu
Formal analysis: Hui Li, Xiaodong Liu
Funding acquisition: Hui Li, Chi Wang
Investigation: Hui Li, Xiaodong Liu, Chi Wang
Methodology: Hui Li, Xiaodong Liu
Project administration: Hui Li, Chi Wang
Resources: Hui Li
Software: Xiaodong Liu
Supervision: Hui Li, Chi Wang
Validation: Xiaodong Liu
Visualization: Xiaodong Liu
Writing – original draft: Xiaodong Liu
Writing – review & editing: Hui Li, Xiaodong Liu, Chi Wang

Abstract Spacecraft surface charging, an important issue in space weather research, is investigated in this study for its susceptibility to Alfvén waves (AW) during geomagnetic storms. The investigation reveals a pronounced increase in spacecraft charging risk in geosynchronous orbit, particularly in the recovery phase of these storms. Although spacecraft potential is inversely related to southward interplanetary magnetic field and solar wind velocity, these correlations are insufficient to account for the observed variances. A marked prevalence of AW during the recovery phase was identified, with AW-influenced solar wind correlating to more negative satellite surface potentials. In particular, an enhancement of the AW amplitude is linked to a higher potential of the satellite. The correlation between heightened AW occurrence, elevated electron temperatures, and thermal velocities in geosynchronous orbit, especially on the night side, is also established. These findings highlight the exacerbating influence of AW on spacecraft charging risks during the recovery phase of geomagnetic storms, underscoring the urgent need for improved monitoring and mitigation strategies.

Plain Language Summary Spacecraft charging, a significant space weather issue, can affect satellite operations and safety. This study explores the impact of solar wind disturbances known as Alfvén waves on the charging of geosynchronous satellites during geomagnetic storms. We discovered that satellites are more likely to have lower surface potentials during the recovery phase of storms than during the main phase. Factors such as the direction of the interplanetary magnetic field and the solar wind speed play a role in this phenomenon, but they do not fully account for the changes observed. Our findings indicate that Alfvén waves are more prevalent during the recovery phase, contributing to the negative charging of the satellites. In particular, an increase in the amplitude of these waves reduces the negativity of the satellite potential. These findings highlight the crucial role of Alfvén waves in heightening the risk of spacecraft charging during geomagnetic storms, suggesting the need for enhanced monitoring and strategies to mitigate these risks.

1. Introduction

Spacecraft surface charging, the process that generates a potential difference between the spacecraft surface and the ambient plasma, is a significant issue in space weather research (Garrett, 1981). This phenomenon can affect the accuracy of space plasma measurements, damage instrumentation, and impact navigation systems. Studies have shown that a staggering 75% of failures in geosynchronous orbit spacecraft are related to surface charging and discharging (Xu et al., 2013).

In geosynchronous orbit, spacecraft charging is particularly significant due to the potential for environmental plasma temperatures to reach keV or higher (S. T. Lai & Della-Rose, 2001; S. T. Lai & Tautz, 2006). During geomagnetic storms and substorms, magnetic reconnection in the magnetotail can accelerate electrons, increasing their energy to keV levels, which results in the spacecraft becoming negatively charged (Bodeau, 2015; DeForest, 1972; Sarno-Smith et al., 2016). Thermal electrons from the magnetotail drift toward the dayside, making them more likely to appear from midnight to dawn in geosynchronous orbit (Thomsen et al., 2013). Additionally, surface charging is influenced by currents from photo-electron emission and secondary electron emission (Wu et al., 2000).

Solar wind conditions and geomagnetic activity are important in affecting the spacecraft charging environment (Ganushkina et al., 2021; Matéo-Vélez et al., 2018). For example, Thomsen et al. (2013) analyzed data from six geosynchronous spacecraft over 13 years, revealing that the likelihood of spacecraft surface charging increases during periods of higher Kp index, in the sector from midnight to dawn, during equinoctial seasons and the

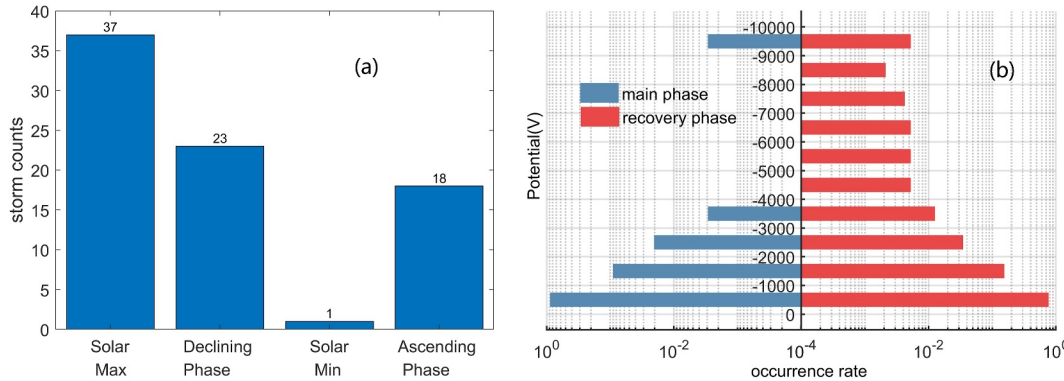

Figure 1. (a) Distribution of the geomagnetic storms across different phases of the solar cycle (b) Distribution of spacecraft potentials during geomagnetic storms in geosynchronous orbit. Blue represents the main phase, and red represents the recovery phase.

declining phase of the solar activity cycle. Sarno-Smith et al. (2016) found that elevated electron energy fluxes and pressures manifest during spacecraft charging intervals. Degtjarev et al. (2000) suggested that an increase in electron flux in the geosynchronous orbit is highly correlated with the increase in solar wind dynamic pressure. The negative surface potential of spacecraft during the recovery phase of geomagnetic storms caused by corotating interaction region events (CIRs) persists for a longer duration, with the plasma sheet temperature remaining elevated for a longer time during CIRs than during interplanetary coronal mass ejections (ICMEs). Recently, Fu et al. (2024) discovered that surface charging potentials without eclipse exhibit a negative threshold dictated by the intensity of substorms.

Beyond these influences, the reconnection between the southward magnetic field component of solar wind Alfvén waves (AWs) and the magnetospheric magnetic field is also used to explain solar wind-magnetosphere coupling (D'Amicis et al., 2020). Alfvén waves are transverse magnetohydrodynamic (MHD) waves that propagate along magnetic field lines in plasma, representing a common fluctuation in the solar wind and widely observed in high-speed solar wind streams. Numerous studies have demonstrated their impact on geomagnetic activity, including extend the duration of storm recovery phase (Telloni et al., 2021), modulate the morphology of recovery phase (Li et al., 2024), and drive High-Intensity Long Duration Continuous AE Activity Storms (HILDCAAS) (Tsurutani & Gonzalez, 1987). These findings indicate the importance of Alfvén waves in the risk assessment of spacecraft charging, yet this aspect has not received much research attention. Therefore, the primary objective of this paper is to explore whether the presence of Alfvén waves affects the charging of spacecraft in geosynchronous orbit and to elucidate the extent and manner of their influence.

2. Higher Charging Risk During Storm Recovery Phase

In geosynchronous orbit, severe spacecraft surface charging phenomena are more likely to occur during geomagnetic storms (Matéo-Vélez et al., 2018). Therefore, 79 geomagnetic storms from 1997 to 2007 are selected for this study. We define the phases of geomagnetic storms based on the variations of the Dst index, following the criteria established in our previous research Li et al. (2024): Main phase is the period from the onset of a rapid decrease in the Dst index to its minimum value. Recovery phase is the period from the minimum Dst value until it recovers to −20 nT. As shown in Figure 1a, the number of storms occurring during the solar minimum, maximum, ascending, and descending phases are 1, 37, 18, and 23, respectively. We also performed statistical analysis using −10 nT as the cutoff of storm recovery phase, and the results remain. These storm lists and the corresponding results are available in data set (Liu, 2025).

We conduct a statistical analysis of the charging occurrences of the LANL-97A spacecraft located in geosynchronous orbit during these events, along with environmental electron temperatures and corresponding solar wind conditions, including the occurrence rates of Alfvén waves. The solar wind speed and Interplanetary Magnetic Field (IMF) Bz data are obtained from the one-hour resolution OMNI data set (King & Papitashvili, 2005). The identification method for Alfvén waves is adopted from Li et al. (2016) and can identify Alfvén waves for each hourly interval, with periods ranging from 10 to 1,000 s. The Magnetospheric Plasma Analyzer (MPA) measures

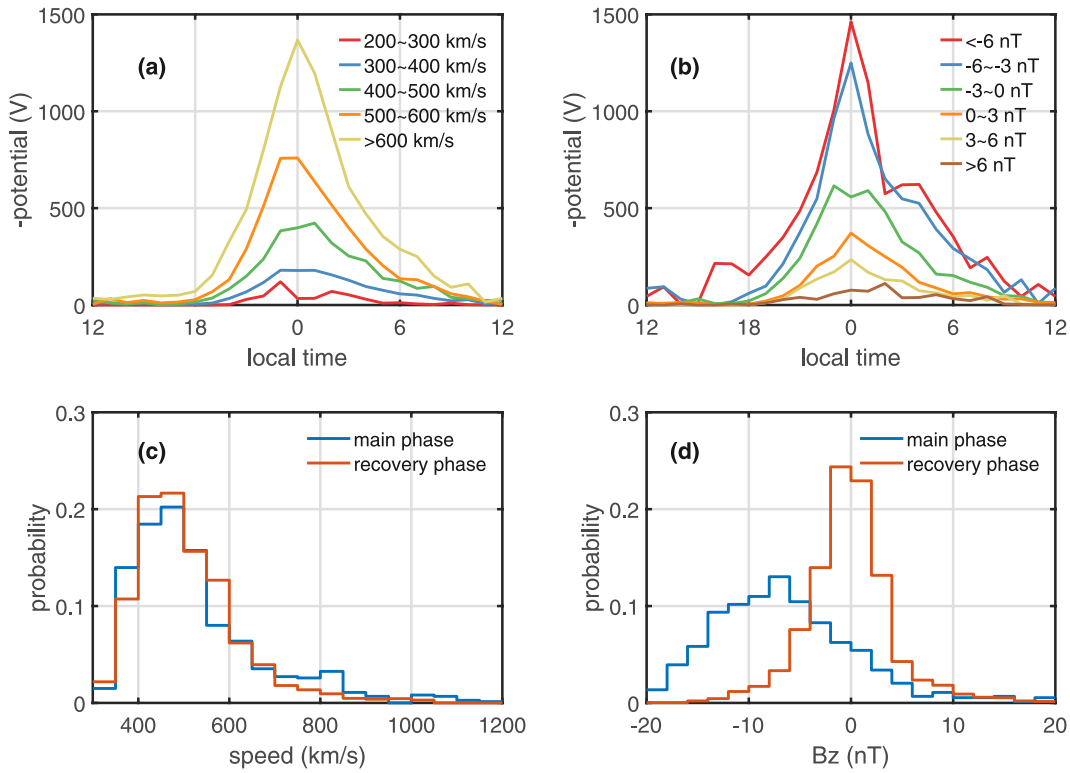

Figure 2. Local time distribution of the spacecraft potential for different (a) solar wind speed and (b) IMF Bz. Probability distribution of solar wind condition for the main and recovery phase (c) solar wind speed and (d) IMF Bz.

the 3D energy-per-charge distributions of ions and electrons. These data, especially the low-energy ion cutoff in the proton spectra, can be used to extract the "shift of ion line" and infer the spacecraft potential. The original resolution of the potential data from MPA instruments is 86 s. To align with other data, we averaged the potential values over one-hour intervals (Bame et al., 1993). We note that the average duration of the main phase in our data set is approximately 14.38 hr, while the recovery phase lasts around 75.05 hr. Considering the difference in duration between the main and recovery phases, our statistical analysis is based on occurrence probability rather than cumulative counts, which normalizes for differences in phase duration and ensures a consistent basis for comparison.

Figure 1b shows the distinct distribution of the measured spacecraft potential from the LANL-97A MPA during geomagnetic storms in geosynchronous orbit. The blue and red represent the main and recovery phases, respectively. For spacecraft potentials more negative than −1,000 V, the occurrence rate during the main and recovery phases are closely matched, at 95.13% and 94.26%, respectively. However, for potentials more negative than −1,000 V, the recovery phase exhibits a significantly higher occurrence rate. Specifically, for potentials between −1,000 and −2,000 V, the occurrence rate during the recovery phase is 82.78% higher than during the main phase. This trend continues with potentials between −2,000 and −3,000 V, where the recovery phase's occurrence rate is 64.13% higher. For potentials between −3,000 and −4,000 V, the recovery phase's occurrence rate soars to 318% higher than during the main phase. For the most negative potentials, between −4,000 and −9,000 V, the recovery phase maintains a steady, albeit low, occurrence rate of approximately 0.5%, in contrast to the main phase where no occurrences are recorded.

Figures 2a and 2b present the local time distribution of the spacecraft potential for all publicly available LANL-97A data from 1997 to 2007, calculated by averaging the potential under different solar wind conditions and local times. Distinct colored lines represent different solar wind conditions. The curves exhibit a peak around midnight (LT = 0), with an increasing solar wind speed correlated with higher absolute spacecraft potential values, as shown in Figure 2a. Due to the dawn-ward drift of electrons from the magnetotail, spacecraft potential exhibits an asymmetric distribution around midnight. For instance, in Figure 2a, the average potential absolute value in the

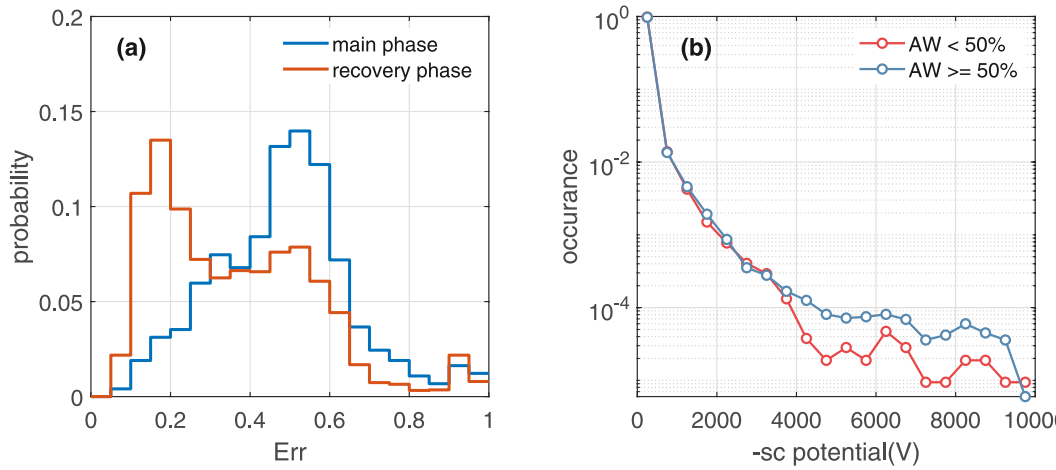

Figure 3. Alfvén waves during storms (a) the probability distribution of average Err value during main phase and recovery phase; (b) the distribution of spacecraft potential under different solar wind Alfvén wave conditions.

dawn sector is higher compared to that in the dusk sector, which is consistent with findings from Choi et al. (2011). As shown in Figure 2b, the local time distribution pattern for IMF Bz is similar, with a more southward IMF Bz leading to greater absolute spacecraft potentials. Ganushkina et al. (2021) found that the velocity of the solar wind serves as a direct indicator of the highest risk for severe surface charging environments, while no clear dependence on IMF Bz has been reported for the occurrence of such severe conditions. Our statistical analysis reveals that when considering all data, not just during high-risk periods for spacecraft potential, both the interplanetary magnetic field Bz and solar wind speed influence the average spacecraft potential.

To ascertain whether the potential differences between the main and recovery phases of magnetic storms, as indicated in Figure 1, are due to solar wind speed and IMF Bz, we conduct a statistical analysis of these parameters during both phases, as depicted in Figures 2c and 2d. Surprisingly, the analysis revealed no significant difference in solar wind speed distribution, with IMF Bz even more southward during the main phase. This finding contradicts the expected trend from Figures 2a and 2b, suggesting that factors beyond solar wind speed and magnetic field influence spacecraft potential during storms.

The predominant large amplitude southward IMF during the main phase contrasts with the northward or fluctuating north-south fields during the recovery phase. We hypothesize that north-south fluctuations associated with Alfvén waves, known to prolong the recovery phase, may heighten the charging risk.

3. Dependence on Alfvén Waves: Incidence and Amplitude

Figure 3a illustrates the distribution of high-purity Alfvén waves during all main and recovery phases of geomagnetic storms. The parameter Err serves as a parameter to quantify the "Alfvénicity" of observed fluctuations in the plasma, that is, how closely they resemble ideal Alfvén waves. Generally, the better the Walén relation holds, the more purely Alfvénic the fluctuations are. Chao et al. (2014) suggested that the ratio of standard deviations, together with the correlation coefficient between plasma velocity fluctuations (V) and Alfvén velocity fluctuations (VA), are better parameters for the Walén test. Based on this, Err integrates these key diagnostics into a single parameter (Li et al., 2016):

$$E_{rr} = \frac{1}{8}\left[\|\gamma_c| - 1| + \sum \|\gamma_{ci}| - 1| + \left|\frac{\sigma_{\delta V}}{\sigma_{\delta V_A}} - 1\right| + \sum \left|\frac{\sigma_{\delta V_i}}{\sigma_{\delta V_{Ai}}} - 1\right| \right] \quad (i = x, y, z) \tag{1}$$

where γ_c is the correlation coefficient between all components of the band-passed plasma velocity and Alfvén velocity fluctuations, $\sigma_{\delta V}$ represents the standard deviation of band-passed plasma velocity fluctuations, and $\sigma_{\delta V_A}$ represents the standard deviation of band-passed Alfvén velocity fluctuations. The closer Err is to 0, the better the Walén test is satisfied. In Figure 3a, Alfvén wave is defined by E_{rr} less than 0.3.

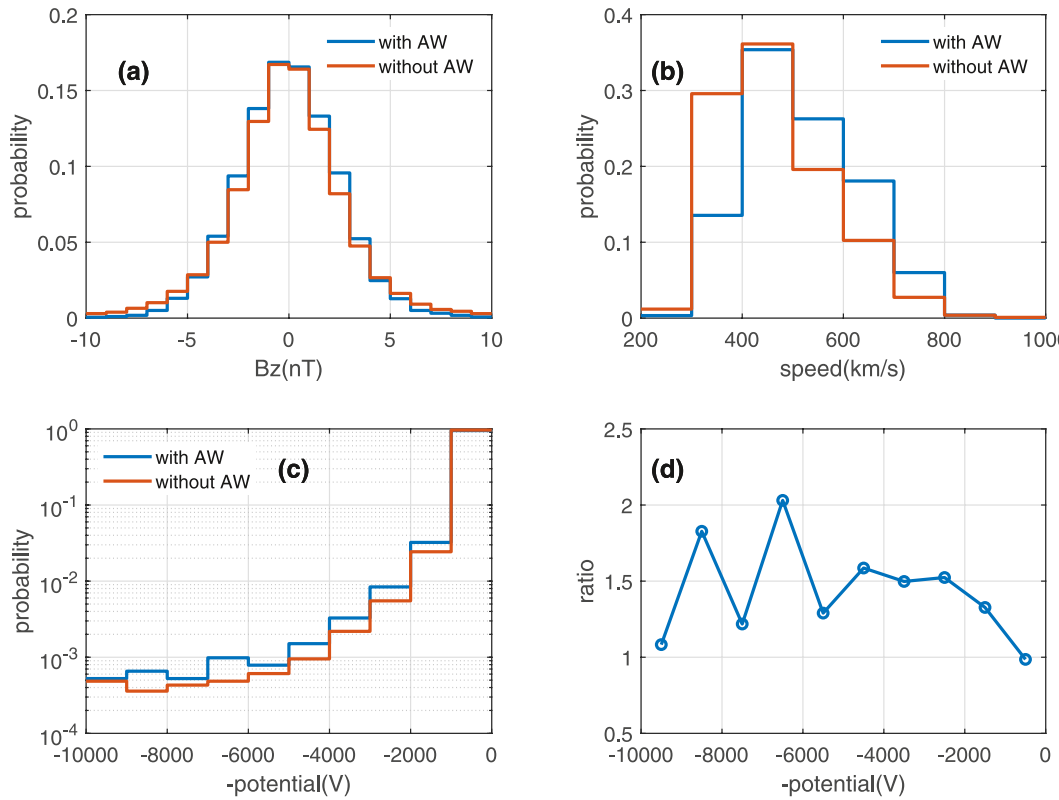

Figure 4. (a) IMF Bz dependence on Alfvén waves occurrence; (b) solar wind speed dependence on Alfvén waves occurrence; (c) Spacecraft potential dependence on Alfvén waves occurrence; (d) the ratio of potential occurrence rates between the solar wind with AW and the solar wind without AW.

It is evident that the recovery phase exhibits a higher occurrence of Alfvén waves, with occurrence rates of approximately 0.1 during the main phase and 0.4 during the recovery phase. Figure 3b further segments the recovery phase based on Alfvén wave occurrence rates, showing that intervals with higher rates, exceeding 50%, are more likely to experience charging below −4,000 V. During recovery phases where the AW occurrence rate exceeds 50%, the incidence of spacecraft potentials dropping below −4,000 V is 2.25 times higher than during recovery phases with an AW occurrence rate below 50%.

To assess whether the influence of Alfvén waves on spacecraft potential persists under various geomagnetic conditions, the entire data set is analyzed to improve the generalizability of the findings. Figures 4a and 4b present the solar wind speed and IMF Bz distributions of AW-type and non-AW-type solar wind, respectively, based on WIND data from 1997 to 2007. AW-type solar wind shows a higher prevalence of speeds above 500 km/s, with both AW-type and non-AW-type solar winds peaking between 400 and 500 km/s. The Bz distribution for both types is near-normal and centered at 0 nT, with AW-type solar wind tending to cluster more closely around 0 nT. By selecting data with speeds between 400 and 500 km/s and Bz between −1 and 1 nT, Figure 4c demonstrates the spacecraft potential distributions under AW-type and non-AW-type solar wind conditions. It is clear that AW-type solar wind is associated with higher spacecraft potentials when other conditions are held constant. Figure 4d plots the ratio of the heights of the red and blue bars from Figure 4c, representing the relative contributions of the two types of solar wind conditions across the range of satellite potentials. Figure 4d shows that in the range of −10,000 to −2,000 V, the proportion of spacecraft potentials corresponding to solar wind conditions with AW is approximately 50% higher than that of solar wind without AW. In the range of −2,000 to −1,000 V, this value is 32.7%. We also extended the solar wind speed range from 400–500 km/s to 300–600 km/s and the IMF Bz range from −1 1 to −2 2 nT. The results show that AW-type solar wind remains more likely to induce spacecraft potentials below −1,000 V, consistent with our previous findings. However, the contrast of potential occurrence between the two types of solar wind is reduced under these broader conditions.

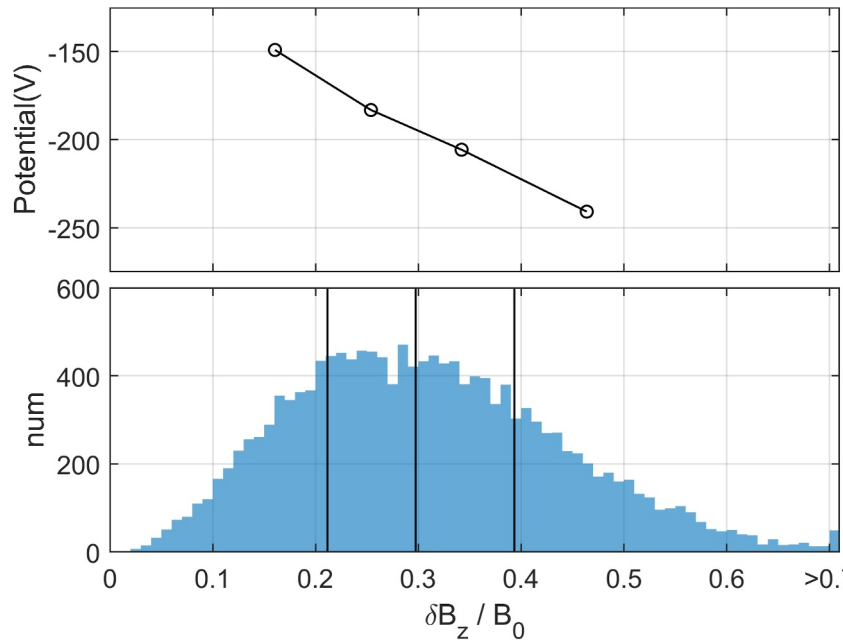

Figure 5. Surface potential dependence on Alfvén waves amplitude.

In addition to the occurrence of Alfvén waves affecting the potential of geosynchronous spacecraft, we find that the amplitude of these waves also plays a significant role. Figure 5 presents our findings, where the bottom panel displays the distribution of AW amplitudes in the solar wind. The amplitude is determined as the standard deviation of the IMF Bz component relative to the background magnetic field strength B_0, following the methodology outlined by Squire et al. (2016).

We categorize the amplitude data into four regions and calculate the average spacecraft potential for each segment. The results, depicted in the top panel of Figure 5, reveal a distinct trend: an increase in the amplitude of interplanetary Alfvén waves corresponds to a rise in the negative spacecraft potential. Specifically, for every 0.1 increment in AW amplitude, there is an approximate increase of 30 V in the average negative spacecraft potential.

4. How AWs Affect the Surface Potential

The electrostatic equilibrium in spacecraft surface potential is a result of the balance of currents entering and exiting the satellite within the plasma environment (S. Lai, 2003). The main currents include electron current, ion current, and photoelectric current, with the latter being influenced by solar photons and the material of the spacecraft's surface. Due to the much higher velocity of electrons compared to ions, geosynchronous spacecraft are more prone to negative charging (S. T. Lai & Della-Rose, 2001). Persistent Alfvén fluctuations in the solar wind, especially during the recovery phase, can lead to continuous substorm activity, enabling hot electrons from the magnetotail to reach the geosynchronous environment and enhance satellite negative charging.

Since the duration of the main phase is insufficient to ensure a uniform distribution across local time, data scarcity may reduce the statistical significance. Therefore, we focus exclusively on the recovery phase in this section. Figure 6 illustrate the local time distribution of low-energy electron thermal speed during the recovery phase of magnetic storms under conditions with and without Alfvén waves. The thermal velocity is given by $V_{\text{the}} = \sqrt{\frac{T_e}{M_e}}$, where T_e is electron temperature and M_e is electron mass. The presence of AWs is defined by an occurrence rate exceeding 70%, while an absence is indicated by a rate below 70%. The figures reveal that electron thermal speed in geosynchronous orbit are elevated during recovery phases with AWs, with the nightside showing a particularly significant increase.

S. T. Lai et al. (2017) noted that when ambient electrons follow a Maxwellian distribution, the spacecraft potential increases almost linearly with rising temperature. These observations suggest that AWs substantially influence

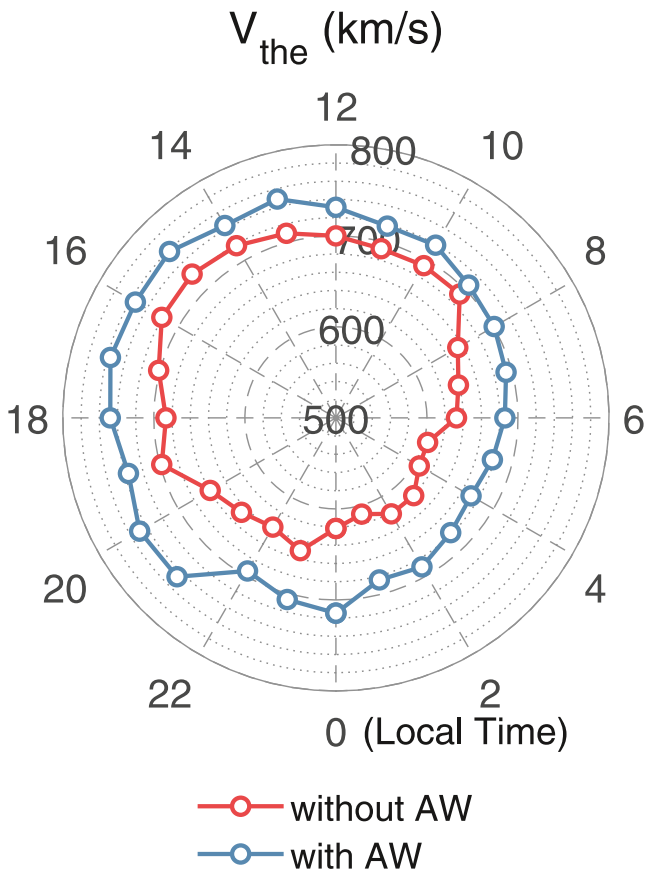

Figure 6. Local time distribution of the electron thermal velocity under solar wind with and without Alfvén Waves.

the electron environment in geosynchronous orbit, especially at night, which may have implications for spacecraft surface charging and operational safety.

5. Summary

This study aims to demonstrate the critical role of interplanetary Alfvén waves in increasing the risk of geosynchronous spacecraft charging. According to Tsurutani et al. (1990, 2006), the magnetic reconnection associated with Alfvén waves causes continuous plasma injections from the plasma sheet into the magnetosphere, which may influence spacecraft charging behavior. In the majority of substorms, the growth phase controlled by solar wind conditions lasts less than 2 hr, which is shorter than either storm phase (Li et al., 2013). Besides using a normalized probability distribution for statistical analysis, this physical mechanism also strengthens the argument that the difference in duration between the main phase and recovery phase does not bias the analysis.

Our main findings are as follows:

1. The occurrence of very negative spacecraft potentials is higher during the recovery phase of a geomagnetic storm compared to the main phase.
2. Statistical studies reveal that spacecraft potential is inversely proportional to the southward magnetic field strength and solar wind speed. However, the Bz and speed distributions during the main and recovery phases do not fully explain the observed potential differences.
3. The recovery phase exhibits a higher occurrence of Alfvén waves compared to the main phase. AW-type solar wind is associated with more negative spacecraft potentials, and an increasing AW amplitude leads to higher spacecraft potentials.
4. Higher AW occurrence rates during magnetic storms are accompanied by higher electron temperatures in geosynchronous orbit, potentially contributing to more severe charging conditions.

These findings underscore the importance of monitoring and mitigating the risks associated with spacecraft charging, particularly during the recovery phase of geomagnetic storms. The higher occurrence of severe charging events during this phase poses greater risks to spacecraft operation and longevity. Our study highlights the need for improved predictive models and protective measures to safeguard spacecraft in geosynchronous orbit, especially considering the potential for extended recovery phases influenced by Alfvén waves. By comparing the statistical results of spacecraft potential under two types of solar wind conditions—with similar speed and Bz but differing in the occurrence of Alfvén waves—we reinforce the credibility of the conclusion that Alfvénic solar wind leads a higher risk for satellite charging. Statistical analysis of the entire data set further confirms that the amplitude of Alfvén waves significantly influences the satellite potential. Future research should focus on further elucidating the mechanisms behind these charging phenomena and developing strategies to mitigate their impact on spacecraft systems.

Data Availability Statement

Publicly available data sets were analyzed in this study. The Wind data from https://cdaweb.gsfc.nasa.gov/pub/data/wind/; Dst data from https://wdc.kugi.kyoto-u.ac.jp/; LANL data from https://cdaweb.gsfc.nasa.gov/pub/data/lanl/. And We provide the list of geomagnetic storms, along with the Alfvén wave and spacecraft potential data used in this study in the data set Liu (2025).

Acknowledgments
We thank NASA's Space Physics Data Facility for providing the LANL data and the Wind data (https://spdf.gsfc.nasa.gov) and the World Data Center for Geomagnetism, Kyoto, for providing the Dst data (https://wdc.kugi.kyoto-u.ac.jp/). This work is supported by NNSFC Grants (42374198, 42188101), the project of Civil Aerospace "14th Five Year Plan" Preliminary Research in Space Science (D010202, D010301). H. Li is also supported by the International Partnership Program of CAS (Grant 183311KYSB20200017), the Beijing Municipal Science & Technology Commission (Grant Z221100002722006), and partly by the Specialized Research Fund for State Key Laboratories of China.

References

Bame, S. J., McComas, D. J., Thomsen, M. F., Barraclough, B. L., Elphic, R. C., Glore, J. P., et al. (1993). Magnetospheric plasma analyzer for spacecraft with constrained resources. *Review of Scientific Instruments*, *64*(4), 1026–1033. https://doi.org/10.1063/1.1144173

Bodeau, M. (2015). Review of better space weather proxies for spacecraft surface charging. *IEEE Transactions on Plasma Science*, *43*(9), 3075–3085. https://doi.org/10.1109/TPS.2015.2441038

Chao, J. K., Hsieh, W.-C., Yang, L., & Lee, L. C. (2014). Walén test and de Hoffmann-teller frame of interplanetary large-amplitude Alfvén waves. *The Astrophysical Journal*, *786*(2), 149. https://doi.org/10.1088/0004-637X/786/2/149

Choi, H.-S., Lee, J., Cho, K.-S., Kwak, Y.-S., Cho, I.-H., Park, Y.-D., et al. (2011). Analysis of geo spacecraft anomalies: Space weather relationships: Space weather effects on geo spacecraft anomalies. *Space Weather*, *9*(6). https://doi.org/10.1029/2010SW000597

D'Amicis, R., Telloni, D., & Bruno, R. (2020). The effect of solar-wind turbulence on magnetospheric activity. *Frontiers in Physics*, *8*, 604857. https://doi.org/10.3389/fphy.2020.604857

DeForest, S. E. (1972). Spacecraft charging at synchronous orbit. *Journal of Geophysical Research*, *77*(4), 651–659. https://doi.org/10.1029/JA077i004p00651

Degtjarev, V. I., Popov, G. V., & Johnstone, A. D. (2000). Solar wind control of spacecraft charging conditions in geostationary orbit during magnetic storms. *Advances in Space Research*, *26*(1), 37–40. https://doi.org/10.1016/S0273-1177(99)01024-8

Fu, Z., Su, Z., Miao, B., Wu, Z., Li, Y., Liu, K., et al. (2024). A substorm-dependent negative limit of non-eclipse surface charging of a Chinese geosynchronous satellite. *Space Weather*, *22*(2), e2023SW003780. https://doi.org/10.1029/2023SW003780

Ganushkina, N. Y., Swiger, B., Dubyagin, S., Matéo-Vélez, J.-C., Liemohn, M. W., Sicard, A., & Payan, D. (2021). Worst-case severe environments for surface charging observed at LANL satellites as dependent on solar wind and geomagnetic conditions. *Space Weather*, *19*(9), e2021SW002732. https://doi.org/10.1029/2021SW002732

Garrett, H. B. (1981). The charging of spacecraft surfaces. *Reviews of Geophysics*, *19*(4), 577–616. https://doi.org/10.1029/RG019i004p00577

King, J. H., & Papitashvili, N. E. (2005). Solar wind spatial scales in and comparisons of hourly wind and ace plasma and magnetic field data. *Journal of Geophysical Research*, *110*(A2). https://doi.org/10.1029/2004JA010649

Lai, S. T. (2003). A critical overview on spacecraft charging mitigation methods. *IEEE Transactions on Plasma Science*, *31*(6), 1118–1124. https://doi.org/10.1109/TPS.2003.820969

Lai, S. T., & Della-Rose, D. J. (2001). Spacecraft charging at geosynchronous altitudes: New evidence of existence of critical temperature. *Journal of Spacecraft and Rockets*, *38*(6), 922–928. https://doi.org/10.2514/2.3764

Lai, S. T., Martinez-Sanchez, M., Cahoy, K., Thomsen, M. F., Shprits, Y., Lohmeyer, W., & Wong, F. K. (2017). Does spacecraft potential depend on the ambient electron density? *IEEE Transactions on Plasma Science*, *45*(10), 2875–2884. https://doi.org/10.1109/TPS.2017.2751002

Lai, S. T., & Tautz, M. (2006). High-level spacecraft charging in eclipse at geosynchronous altitudes: A statistical study. *Journal of Geophysical Research*, *111*(A9), A09201. https://doi.org/10.1029/2004JA010733

Li, H., Liu, X., & Wang, C. (2024). How solar wind controls the recovery phase morphology of intense magnetic storms. *Journal of Geophysical Research: Space Physics*, *129*(3), e2023JA032057. https://doi.org/10.1029/2023JA032057

Li, H., Wang, C., Chao, J. K., & Hsieh, W. C. (2016). A new approach to identify interplanetary alfvén waves and to obtain their frequency properties. *Journal of Geophysical Research: Space Physics*, *121*(1), 42–55. https://doi.org/10.1002/2015JA021749

Li, H., Wang, C., & Peng, Z. (2013). Solar wind impacts on growth phase duration and substorm intensity: A statistical approach. *Journal of Geophysical Research: Space Physics*, *118*(7), 4270–4278. https://doi.org/10.1002/jgra.50399

Liu, X. D. (2025). Enhanced spacecraft charging risks by interplanetary Alfven waves during geomagnetic storms [Dataset]. *Zenodo*. https://doi.org/10.5281/zenodo.15221717

Matéo-Vélez, J.-C., Sicard, A., Payan, D., Ganushkina, N., Meredith, N. P., & Sillanpää, I. (2018). Spacecraft surface charging induced by severe environments at geosynchronous orbit. *Space Weather*, *16*(1), 89–106. https://doi.org/10.1002/2017SW001689

Sarno-Smith, L. K., Larsen, B. A., Skoug, R. M., Liemohn, M. W., Breneman, A., Wygant, J. R., & Thomsen, M. F. (2016). Spacecraft surface charging within geosynchronous orbit observed by the Van Allen Probes. *Space Weather*, *14*(2), 151–164. https://doi.org/10.1002/2015SW001345

Squire, J., Quataert, E., & Schekochihin, A. A. (2016). A stringent limit on the amplitude of Alfvénic perturbations in high-beta low-collisionality plasmas. *The Astrophysical Journal Letters*, *830*(2), L25. https://doi.org/10.3847/2041-8205/830/2/L25

Telloni, D., D'Amicis, R., Bruno, R., Perrone, D., Sorriso-Valvo, L., Raghav, A. N., & Choraghe, K. (2021). Alfvénicity-related long recovery phases of geomagnetic storms: A space weather perspective. *The Astrophysical Journal*, *916*(2), 64. https://doi.org/10.3847/1538-4357/ac071f

Thomsen, M. F., Henderson, M. G., & Jordanova, V. K. (2013). Statistical properties of the surface-charging environment at geosynchronous orbit: Surface charging at geosynchronous orbit. *Space Weather*, *11*(5), 237–244. https://doi.org/10.1002/swe.20049

Tsurutani, B. T., & Gonzalez, W. D. (1987). The cause of high-intensity long-duration continuous ae activity (Hildcaas): Interplanetary Alfvén wave trains. *Planetary and Space Science*, *35*(4), 405–412. https://doi.org/10.1016/0032-0633(87)90097-3

Tsurutani, B. T., Gonzalez, W. D., Gonzalez, A. L. C., Guarnieri, F. L., Gopalswamy, N., Grande, M., et al. (2006). Corotating solar wind streams and recurrent geomagnetic activity: A review. *Journal of Geophysical Research*, *111*(A7), A07S01. https://doi.org/10.1029/2005JA011273

Tsurutani, B. T., Gould, T., Goldstein, B. E., Gonzalez, W. D., & Sugiura, M. (1990). Interplanetary Alfvén waves and auroral (substorm) activity: Imp 8. *Journal of Geophysical Research*, *95*(A3), 2241–2252. https://doi.org/10.1029/JA095iA03p02241

Wu, J. G., Eliasson, L., Lundstedt, H., Hilgers, A., Andersson, L., & Norberg, O. (2000). Space environment effects on geostationary spacecraft: Analysis and prediction. *Advances in Space Research*, *26*(1), 31–36. https://doi.org/10.1016/S0273-1177(99)01023-6

Xu, B., Wu, Z., & Zhang, P. (2013). Study on effect of space environment on surface charging of spacecraft. *Journal of Physics: Conference Series*, *418*, 012042. https://doi.org/10.1088/1742-6596/418/1/012042